MOLECULAR PHYSICS, 1992, VOL. 76, NO. 5, 1147–1156

On the use of variational wavefunctions in calculating vibrational band intensities

By C. RUTH LE SUEUR, STEVEN MILLER, JONATHAN TENNYSON
Department of Physics and Astronomy, University College London, Gower St, London WC1E 6BT, UK

and BRIAN T. SUTCLIFFE
Department of Chemistry, University of York, York YO1 5DD, UK

(*Received 19 December 1991; accepted 6 February 1992*)

It is shown that vibrational band intensities calculated using variational wavefunctions and dipole surfaces give results which depend on how the Cartesian axes of the dipole surface are defined. It is suggested that the most consistent definition of these axes uses the rules proposed by Eckart for separating ro-vibrational motion. The consequences of this choice of axis system for the calculated band intensities of H_2S, LiNC and H_3^+, and the apparent validity of Hönl–London factors are discussed. Computed band intensities are presented for H_2S, HDS and D_2S which correct previous literature values.

1. Introduction

The intensity of a series of ro-vibrational transitions ($V'J'-V''J''$) are often characterized in terms of a single parameter which is a constant for the vibrational transition ($V'-V''$) under consideration. This parameter is known as the vibrational band intensity. The intensity of each ro-vibrational line in this band is then characterized by a purely algebraic factor usually called a Hönl–London factor [1]. Although the assumptions underlying this method of characterizing intensities sometimes break down, for instance when there is intensity stealing between nearby ro-vibrational levels, vibrational band intensities are of great use as they allow a lot of data to be represented by a single parameter. They are thus a common currency which is widely used to assess whether a particular band may be intense enough to be observed or to estimate the lifetime of a vibrationally excited state.

Within the harmonic oscillator approximation, vibrational band intensities can be calculated from the derivative of the dipole at equilibrium [2]. Recently, however, a number of ro-vibrational methods have been developed which go considerably beyond the harmonic oscillator approximation. These methods use internal coordinates, Hamiltonians which are often exact within the Born–Oppenheimer approximation, and the variational principle to derive accurate representations of ro-vibrational wavefunctions. The internal coordinate system used usually dictates the choice of axis embedding for these calculations. Since one is not constrained to produce a good separation between vibrational and rotational motion, the coordinate system (and hence the axis embedding) tend, however, to be chosen with regard to the chemistry of the molecule rather than to produce a good separation of vibrational and rotational motion. Such methods can be extended to calculate the intensity of individual ro-vibrational transitions [3–5] but for obvious reasons of compactness, a number of

authors have chosen to use rotationless ($J = 0$) wavefunctions from variational calculations and internal coordinate representations of the dipole surface to compute vibrational band intensities directly; see for example studies on H_2S [6–8] and HCN [9, 10].

As far as we can tell, none of these previous studies has considered explicitly the orientation of the dipole axes when computing vibrational band intensities. In this work we show that the results obtained depend on the orientation chosen. Since obtaining accurate band intensities is dependent on a good separation of rotational and vibrational motion, we suggest that a consistent treatment should use axes given by the Eckart conditions [11]. We demonstrate the effect of this by performing a series of calculations on H_2S, LiNC and H_3^+. We present vibrational band intensities for H_2S and its isotopomers which correct previously published values.

2. Theory

The probability of the transition $\Psi' \leftarrow \Psi''$ is given by $|\langle \Psi' | \boldsymbol{\mu}^S | \Psi'' \rangle|^2$ if the transition is actuated by the influence of the electric dipole $\boldsymbol{\mu}^S$.

In general a body-fixed wavefunction $\Psi(JMV)$ for an N-atomic molecule is given by

$$\Psi(JMV) = \left(\frac{2J+1}{8\pi^2}\right)^{1/2} \sum_{k,v} c_v^{JkV} \phi_v^{Jk}(\boldsymbol{q}) |JMk\rangle. \tag{1}$$

In other words, $\Psi(JMV)$ is given as a linear combination of products of angular momentum eigenfunctions and vibrational basis functions ϕ_v^{Jk} expressed with respect to $3N - 6$ internal coordinates, $\boldsymbol{q}$. In most variational procedures the ϕ are themselves further expanded as products of functions in one or more internal coordinates, and the angular momentum functions are written in terms of Wigner $\mathscr{D}$-functions. The exact choice of how $|JMk\rangle$ relates to $\mathscr{D}^J_{M,k}(\boldsymbol{\Omega})$ may vary between workers—we choose to use $|JMk\rangle \equiv (-1)^k \mathscr{D}^{J*}_{M,-k}$—but in any case this only leads to differences in phase factors in the following treatment. In (1), k is the projection of J, the rotational angular momentum, along the body-fixed z axis, and needs to be considered as indicated if a smooth transition between linear and strongly bent geometries is desired.

In the absence of external magnetic fields all space-fixed directions are equivalent and so states $\Psi(JMV)$ with differing M are degenerate. The line strength S_{fi} for a given transition is given by summing the transition probability over all M' and M'' states. The equivalence of all space-fixed axes also means that the total probability is three times the transition probability actuated by a dipole acting only in the space-fixed z direction. The line strength can therefore be written as

$$S_{\text{fi}} = 3\frac{(2J'+1)(2J''+1)}{(8\pi^2)^2} \left| \sum_{\substack{M',M'' \\ k',v',k'',v''}} (-1)^{k'+k''} c_{v'}^{J'k'V'*} c_{v''}^{J''k''V''} \langle \mathscr{D}^{J'*}_{M',-k'} \phi_{v'}^{J'k'} | \mu_z^S | \mathscr{D}^{J''*}_{M'',-k''} \phi_{v''}^{J''k''} \rangle \right|^2, \tag{2}$$

where we have substituted for $|JMk\rangle$ as described above.

It is advantageous, when evaluating (2), to express μ_z^S in terms of the dipole referred to the body-fixed axes (μ_x^B, μ_y^B, μ_z^B). This may be done quite simply by substituting

$$\mu_0^S = \sum_l \mathscr{D}^{1*}_{0,l} \mu_l^B, \tag{3}$$

whilst remembering that

$$\mu_1 = -\frac{1}{\sqrt{2}}(\mu_x + i\mu_y),\ \mu_0 = \mu_z,\ \mu_{-1} = \frac{1}{\sqrt{2}}(\mu_x - i\mu_y), \tag{4}$$

into the above expression. All the components of $\boldsymbol{\mu}$ in (4) refer to body-fixed axes, but we have dropped the superscript B for clarity. This enables the separation of the integral into a sum of several products of integrals

$$S_{\mathrm{fi}} = 3\frac{(2J'+1)(2J''+1)}{(8\pi^2)^2}\left|\sum_{\substack{M',M''\\k',\nu',k'',\nu''}}\sum_{l}(-1)^{k'+k''}c_{\nu'}^{J'k'V'*}c_{\nu''}^{J''k''V''}\langle\mathscr{D}^{J'}_{M',-k'}|\mathscr{D}^{1}_{0,l}|\mathscr{D}^{J''}_{M'',-k''}\rangle^*\right.$$
$$\left.\times\langle\phi_{\nu'}^{J'k'}|\mu_l^{\mathrm{B}}|\phi_{\nu''}^{J''k''}\rangle\right|^2. \tag{5}$$

The integral over the angular coordinates $\boldsymbol{\Omega}$ in each pair may then be evaluated analytically [13]

$$\langle\mathscr{D}^{J'}_{M',-k'}|\mathscr{D}^{1}_{0,l}|\mathscr{D}^{J''}_{M'',-k''}\rangle = (-1)^{M'+k'}8\pi^2\begin{pmatrix}J' & 1 & J''\\ -M' & 0 & M''\end{pmatrix}\begin{pmatrix}J' & 1 & J''\\ k' & l & -k''\end{pmatrix}. \tag{6}$$

The first $3j$ symbol, which is common to the whole of the expression, may be factored out and, using

$$\sum_{M',M''}\begin{pmatrix}J' & 1 & J''\\ -M' & 0 & M''\end{pmatrix}^2 = \frac{1}{3}, \tag{7}$$

the line strength can be written as

$$S_{\mathrm{fi}} = (2J'+1)(2J''+1)$$
$$\times\left|\sum_{k',\nu',k'',\nu''}\sum_{l}(-1)^{k'}c_{\nu'}^{J'k'V'*}c_{\nu''}^{J''k''V''}\begin{pmatrix}J' & 1 & J''\\ k' & l & -k''\end{pmatrix}\langle\phi_{\nu'}^{J'k'}|\mu_l^{\mathrm{B}}|\phi_{\nu''}^{J''k''}\rangle\right|^2. \tag{8}$$

If the vibrational and rotational parts of the motion are well separated, it should be possible to choose the components of the wavefunction so that it simplifies to

$$\Psi(JMV) = \left(\sum_{\nu}a_{\nu}^{V}\phi_{\nu}(\boldsymbol{q})\right)\left(\sum_{k}b^{Jk}|JMk\rangle\right). \tag{9}$$

Precisely how to achieve this separation was first shown by Eckart [11], who derived a set of conditions which an internal axis system must obey in order for the vibration–rotation Hamiltonian to have, as good approximate eigenstates, products of the above type. Methods for identifying the Eckart axis system and embedding the molecule within it have been well covered by, among others, Bunker [12] and Wilson, Decius and Cross [2]. In the limit of small displacements from equilibrium, the above separation is exact. It follows then that

$$S_{\mathrm{fi}} = (2J'+1)(2J''+1)$$
$$\times\left|\sum_{l}\sum_{\nu',\nu''}a_{\nu'}^{V'*}a_{\nu''}^{V''}\langle\phi_{\nu'}|\mu_l^{\mathrm{B}}|\phi_{\nu''}\rangle\sum_{k',k''}(-1)^{k'}b^{J'k'*}b^{J''k''}\begin{pmatrix}J' & 1 & J''\\ k' & l & -k''\end{pmatrix}\right|^2. \tag{10}$$

Working within this approximation, the line strength of a ro-vibrational transition is often factorized as

$$S_{\mathrm{fi}} = S^{\mathrm{Rot}}_{J''J'}S^{\mathrm{Vib}}_{V''V'}, \tag{11}$$

(see, for example, equation (6.129) of reference [15]). Although this factorization is not strictly possible unless for some reason the sum over l is restricted to one value, it is commonly assumed. In this case the vibrational band intensity is defined as

$$S^{\mathrm{Vib}}_{V''V'} = |\langle V'|\boldsymbol{\mu}^{\mathrm{B}}|V''\rangle|^2 = \sum_l |\langle V'|\mu^{\mathrm{B}}_l|V''\rangle|^2. \tag{12}$$

For symmetric top and linear molecules, symmetry considerations dictate that only one component of the transition dipole is ever non-zero and so this factorization is exact. Furthermore, since k is then a good quantum number, the $S^{\mathrm{Rot}}_{J''J'}$ can be calculated algebraically and are frequently tabulated as Hönl–London factors [1, 15]. Leaving aside the question of exactly what should be used as the rotational factors for a general asymmetric top, it is clear that by using this approximation to obtain vibrational band dipoles and hence intensities, it is possible to obtain a fair idea of how intense the transitions within a vibrational band will be.

The identification of and separation between vibrational and rotational motions is of course fundamental in the use of vibrational band intensities and associated rotational factors. What appears to have been generally ignored in previous work which used variational wavefunctions and dipole surfaces to calculate $\langle V'|\boldsymbol{\mu}^{\mathrm{B}}|V''\rangle$ is that identifying axes for the body-fixed dipole, $\boldsymbol{\mu}^{\mathrm{B}}$, implicitly also identifies the body-fixed axes for the rotational motion. If these axes are inappropriate then a poor separation between vibrational and rotational motions will result and partitioning between these motions will no longer be valid. This is true even though vibrational wavefunctions are generally obtained from rotationless ($J = 0$) calculations which are independent of axis embeddings [14]. This is because there is no reason why different axis embeddings should give the same values of $|\langle V'|\boldsymbol{\mu}^{\mathrm{B}}|V''\rangle|^2$. As mentioned above, the method of obtaining the best separation of vibrational and rotational motion has previously been outlined by Eckart. By choosing a set of body fixed axes that obey his conditions

$$\sum_i m_i \mathbf{r}^{\mathrm{e}}_i \times \mathbf{r}_i = \mathbf{0}; \qquad \sum_i m_i \mathbf{r}_i = \mathbf{0}, \tag{13}$$

where m_i is the mass and $\mathbf{r}_i$ the position ($\mathbf{r}^{\mathrm{e}}_i$ at equilibrium) of particle i, we hope to obtain more accurate band intensities.

For the particular case of a triatomic, this conversion is easy to make. Taking, without loss of generality, an embedding which forces the molecule to lie in the body-fixed xz plane, satisfies three of the six Eckart conditions immediately. The other three are satisfied by first referring everything to the centre of mass and then to a new set of axes XZ related to the original by a rotation through θ, given by

$$\tan\theta = \frac{\Sigma^3_{i=1} m_i(x^{\mathrm{e}}_i z_i - z^{\mathrm{e}}_i x_i)}{\Sigma^3_{i=1} m_i(x^{\mathrm{e}}_i x_i + z^{\mathrm{e}}_i z_i)}. \tag{14}$$

The sense of this rotation is given by the figure.

Our approach for calculating vibrational band intensities is now clear. If $J = 0$ wavefunctions are chosen, all that needs to be done is to refer to the dipole to the 'Eckart' internal axes as the wavefunction themselves have no axis dependence.

3. Results

To demonstrate the dependence of vibrational band intensities on the embedding chosen for the body fixed axis system, we have computed vibrational band intensities

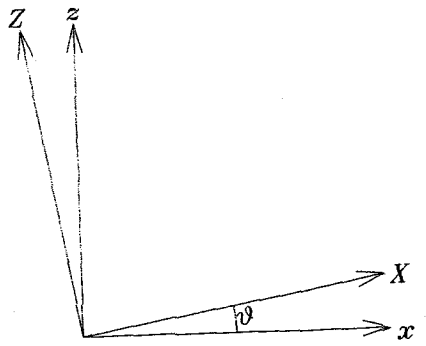

The Eckart axes XZ are related to the original internal axis system xz by a rotation θ.

using the same $J = 0$ wavefunctions for a number of axis embeddings for H_3^+, H_2S and LiNC. These molecules are, respectively, a symmetric top, an asymmetric top and a linear molecule.

We performed calculations on H_3^+ as a function of axis embeddings, using the potential energy and dipole surfaces of Meyer *et al.* (MBB) [16] and the $J = 0$ wavefunctions of Miller *et al.* [17]. H_3^+ has two vibrational fundamentals: an A_1 symmetric stretch, ν_1, and a degenerate, E bend, ν_2.

The symmetry of H_3^+ means that the vibrational band intensities of this ion provide a particularly stringent test of any method. We would expect many vibrational bands to have zero intensity (all A $\leftrightarrow$ A transitions), and E $\leftrightarrow$ E transitions to have two identically intense components. (Our method does not work with the full symmetry of H_3^+, and E state components are calculated in separate even (e) and odd (o) parity calculations [18].)

Calculations were performed on H_3^+ for a number of axis embeddings. The results, see table 1, obtained for the scattering coordinate embedding, where z was taken

Table 1. Vibrational band dipoles for H_3^+ calculated using a scattering coordinate embedding and the Eckart embedding. Band dipoles calculated by Miller *et al.* [17] from the $J = 1 \leftarrow J = 0$ line strengths (see text) are also included for comparison. The dipole components are labelled by whether the bra and ket vibrational wavefunctions are of even (e) or odd (o) parity.

Transition	ω_{if}/cm^{-1}	Scattering embedding μ_{ee}/D†	μ_{oo}/D	μ_{if}/D	Eckart embedding μ_{ee}/D	μ_{oo}/D	μ_{if}/D	[17] μ_{01}/D
$\nu_0 \leftarrow \nu_0$	0·0	0·015	–	0·015	0·001	–	0·001	0·000
$\nu_2 \leftarrow \nu_0$	2521·3	0·162	–	0·229	0·160	–	0·226	0·226
$2\nu_2(l = 0) \leftarrow \nu_2$	2255·7	0·137	–	0·137	0·139	–	0·139	0·131
$2\nu_2(l = 2) \leftarrow \nu_2$	2476·1	0·171	0·168	0·240	0·163	0·164	0·231	0·234
$\nu_2 + \nu_1 \leftarrow \nu_1$	2375·4	0·178	–	0·252	0·174	–	0·246	0·245
$\nu_2 + \nu_1 \leftarrow \nu_2$	3032·4	0·028	0·043	0·051	0·032	0·031	0·045	0·053
$\nu_1 \leftarrow \nu_0$	3178·3	0·004	–	0·004	0·000	–	0·000	0·000
$2\nu_2(l = 2) \leftarrow \nu_0$	4997·4	0·075	–	0·106	0·061	–	0·086	0·089
$3\nu_2(l = 1) \leftarrow \nu_2$	4482·2	0·044	0·079	0·090	0·051	0·049	0·071	0·072
$3\nu_2(l = +3) \leftarrow \nu_2$	4761·2	0·073	–	0·073	0·060	–	0·060	0·061
$3\nu_2(l = -3) \leftarrow \nu_2$	4971·3	–	0·096	0·096	–	0·079	0·079	0·088
$2\nu_2(l = 2) + \nu_1 \leftarrow \nu_1$	4690·3	0·075	–	0·106	0·061	–	0·086	0·089

† 1 D = 3·335 64 × 10^{-30} cm.

Table 2. Vibrational absorption intensities, S_b†, for H_2S obtained using a variety of axis embeddings.

		Absorption intensities/atm^{-1} cm^{-2}			
(v_1, v_2, v_3)	ω_{if}/cm^{-1}	Bisector	Scattering	Radau	Eckart
(0, 1, 0)	1190·4	2·65	2·72	49·50	2·64
(0, 2, 0)	2372·0	0·32	0·33	0·03	0·33
(1, 0, 0)	2620·4	1·40	1·53	1·46	1·40
(0, 0, 1)	2631·0	1·54	67·51	1·09	1·08

† S_b (at 297 K) in atm^{-1} cm^{-2} = 10·245 × ω_{if} (in cm^{-1}) × S_{fi} (in D^2) [7].

parallel to the vector connecting the centre of an H–H diatom to the third H, were typical of those obtained for non-Eckart embeddings. The results presented in table 1 show that the noise (as measured by how different the intensities of such bands are calculated to be, and how intense the bands which should have zero intensity are predicted to be) for the Eckart embedding is much smaller than for a standard triatomic embedding. The Hönl–London factor for the $J = 1 \leftarrow J = 0$ line of a symmetric top within a vibrational band is 1; this was used by Miller *et al.* [17] to compute effective vibrational band dipoles by considering $J = 1 \leftarrow J = 0$ transition dipoles μ_{01} (see column 9 of table 1). These can be compared with μ_{if} from the Eckart embedding to see how very accurate the band intensities resulting from this embedding are.

A number of theoretical studies have been performed on the spectra of H_2S and its isotopomers. We have followed the most recent and accurate of these and used the *ab initio* potential energy and dipole surface of Senekowitsch *et al.* [7] and the $J = 0$ Radau coordinate vibrational wavefunctions of Miller *et al.* [8]. We are only concerned with $J = 0$ wavefunctions, thus we encountered none of the difficulties experienced by Miller *et al.* in symmetrizing their vibrational wavefunctions for H_2S and D_2S.

Table 2 summarizes our results for H_2S and shows that the answers depend on how the axes are defined. It is interesting to note that calculations in which the z axis is oriented along the HSH bisector (column 3) agree well with those in which the z axis is oriented along the scattering coordinate (column 4) for the bend and symmetric stretch, but much less well for the asymmetric stretch where the two axis embeddings begin to differ significantly. Equally, the Radau embedding, in which the z axis is taken along one of the Radau coordinates (and hence nearly parallel to one of the H–S bonds), generally gives very different estimates for the band intensities. We note that Senekowitsch *et al.* [7] used a dipole oriented so that the z axis bisected the HSH angle. Miller *et al.* copied this approach. Our calculations, in column 3 of table 2, reproduce the results of these workers. The final column of this table gives results calculated using the Eckart embedding as outlined above. While both the bisector and scattering embeddings seem to give accurate results for the two bend states given, it is clear that for other excited states, in particular the asymmetric stretch, calculations using these embeddings could be misleading. The Radau embedding, on the other hand, gives a good result for this state, but is inaccurate for the more symmetric states.

Vibrational band intensities were calculated using the dipole surfaces of Senekowitsch *et al.* but with the x and z directions defined in the manner outlined above. Table 3 contains results for the lowest 61 vibrational bands of H_2S and D_2S.

The equivalent transitions in HDS are also shown, although, because of the different ordering of vibrational levels in the mixed isotopomer, a few lower lying transitions have been omitted from the table. Table 3 corrects the results presented in Table V of Senekowitsch *et al.* [7] and Table V of Miller *et al.* [8].

Calculations on LiNC were performed using the *ab initio* potential energy surface of Essers *et al.* [9], dipole surfaces of Brocks *et al.* [20] and $J = 0$ vibrational wavefunctions of Henderson and Tennyson [21], which were obtained using a discrete variable representation (DVR). As in the previous calculations, the CN bond was frozen at its equilibrium value.

Table 4 presents results for LiNC. It is notable that the band intensities obtained using the scattering axis embedding are exactly the same (to all places quoted) as those obtained from the Eckart axis embedding. Presumably the two axis systems differ very little over the normal range of motion. For a linear molecule undergoing a $\Sigma \leftrightarrow \Sigma$ type transition, the Hönl–London factor for a $J = 1 \leftarrow J = 0$ transition is 1. The final columns of table 4 show the results of such a calculation which reproduced the results of Brocks *et al.* [20]. Again the results are in good agreement with vibrational band intensities.

4. Conclusions

We have shown that vibrational band intensities calculated by explicit integration over dipole surfaces with internal coordinate wavefunction depend on how the axes of the dipole surface are defined—a fact that appears to have been ignored in a number of previous calculations. We suggest that the correct axis embedding should maximise the separation between rotational and vibrational motions and hence use the Eckart conditions.

Test calculations on H_3^+, H_2S and LiNC demonstrate the sensitivity of the computed vibrational band intensity to the embedding chosen. For H_3^+ we were only able to obtain reliable band intensities from the $J = 0$ wavefunctions by using the Eckart embedding.

Previous variational calculations [5] have shown differences between transition intensities calculated directly and via vibrational band intensities and Hönl–London factors. As these calculations used incorrectly oriented dipoles to calculate the vibrational band intensities, the conclusion that Hönl–London factors are unreliable should be treated with caution. Indeed for the limited (low J) tests performed here we obtained notably good agreement between band intensities calculated using the Eckart embedding and those obtained by dividing the results of full calculations by the appropriate Hönl–London factors.

Vibrational band intensities give useful information on whether a particular vibrational transition is amenable to observation or how long a vibrational state lives. It is our plan to use our modified vibrational band intensity program to study the intensity of *all* the possible vibrational transitions in the H_3^+ system [22, 23].

We thank James Henderson for helpful discussions during the course of this work. The figure was produced using a program written by A. J. Stone, for which we are grateful. This work was supported by grants from the Science and Engineering Research Council.

Table 3. Vibrational band origins, ω_{if}, and vibrational absorption intensities, S_b, from the ground state for H_2S and isotopomers computed using the Eckart embedding.

Local mode	Normal mode	H_2S		D_2S		HDS	
$[n_1, n_2](v_2)$	(v_1, v_2, v_3)	ω_{if}/ cm^{-1}	S_b/ $atm^{-1}cm^{-2}$	ω_{if}/ cm^{-1}	S_b/ $atm^{-1}cm^{-2}$	ω_{if}/ cm^{-1}	S_b/ $atm^{-1}cm^{-2}$
[0,0] (1)	(0,1,0)	1190.4	2.64(+0)	860.4	1.59(+0)	1039.2	5.95(+0)
[0,0] (2)	(0,2,0)	2372.0	3.29(−1)	1716.6	1.15(−1)	2071.9	1.52(−1)
[0,0] (3)	(0,3,0)	3543.5	4.16(−2)	2568.0	1.09(−2)	3097.3	5.17(−2)
[0,0] (4)	(0,4,0)	4703.7	2.46(−3)	3414.1	3.55(−4)	4114.6	1.35(−3)
[0,0] (5)	(0,5,0)	5851.6	1.27(−4)	4254.7	1.85(−5)	5123.0	8.37(−6)
[0,0] (6)	(0,6,0)	6986.3	2.65(−6)	5089.2	3.61(−7)	6122.0	4.50(−7)
[0,0] (7)	(0,7,0)	8106.9	3.47(−8)	5917.4	5.06(−9)	7110.7	1.16(−8)
[0,0] (8)	(0,8,0)	9212.5	4.71(−10)	6738.8	2.07(−10)	8088.7	5.16(−10)
[0,0] (9)	(0,9,0)	10302.1	5.29(−11)	7553.2	7.39(−12)	9055.9	9.08(−6)
[1,0+] (0)	(1,0,0)	2620.4	1.40(+0)	1900.6	6.66(−1)	1905.9	4.90(−1)
[1,0−] (0)	(0,0,1)	2631.0	1.08(+0)	1912.0	2.84(−1)	2625.6	1.31(+0)
[2,0+] (0)	(2,0,0)	5154.2	3.52(−1)	3760.3	1.16(−1)	3762.2	2.19(−1)
[2,0−] (0)	(1,0,1)	5155.5	6.77(−1)	3763.2	3.13(−1)	4530.2	3.65(−2)
[1,1] (0)	(0,0,2)	5251.2	3.99(−2)	3814.4	4.55(−3)	5155.3	5.00(−1)
[3,0+] (0)	(3,0,0)	7589.3	9.91(−3)	5569.2	1.96(−3)	7058.8	2.65(−3)
[3,0−] (0)	(2,0,1)	7589.4	3.35(−2)	5569.6	1.14(−2)	6384.9	2.02(−3)
[2,1+] (0)	(1,0,2)	7768.4	5.84(−3)	5658.1	9.80(−4)	5569.2	6.53(−3)
[2,1−] (0)	(0,0,3)	7789.3	5.54(−3)	5679.7	1.49(−3)	7591.6	2.30(−2)
[4,0+] (0)	(4,0,0)	9929.0	5.98(−6)	7331.4[a]	2.18(−6)	8912.5	2.32(−7)
[4,0−] (0)	(3,0,1)	9929.0	1.00(−3)	7331.4[a]	2.25(−4)	8189.7	9.99(−5)
[3,1+] (0)	(2,0,2)	10208.3	3.89(−4)	7468.5	5.11(−5)	7326.7	1.47(−4)
[3,1−] (0)	(1,0,3)	10212.0	4.37(−4)	7476.1	7.75(−5)	9562.7	9.53(−8)
[2,2] (0)	(0,0,4)	10308.8	1.59(−5)	7529.6	1.05(−5)	10010.9	1.35(−6)
[1,0+] (1)	(1,1,0)	3794.6	1.78(+0)	2752.5	6.91(−1)	2934.8	1.09(+0)
[1,0−] (1)	(0,1,1)	3799.8	2.28(+0)	2761.3	8.88(−1)	3645.6	1.53(+0)
[1,0−] (2)	(0,2,1)	4960.0	4.53(−2)	3606.4	1.31(−2)	4659.5	1.82(−2)
[1,0+] (2)	(1,2,0)	4960.1	6.38(−3)	3600.2	7.65(−4)	3957.2	1.45(−2)
[1,0−] (3)	(0,3,1)	6110.2	8.74(−4)	4446.8	1.53(−4)	5666.2	8.61(−4)
[1,0+] (3)	(1,3,0)	6115.6	2.08(−3)	4443.3	3.52(−4)	4972.4	1.38(−3)
[1,0−] (4)	(0,4,1)	7249.4	4.92(−5)	5282.0	5.29(−6)	6665.0	4.39(−5)
[1,0+] (4)	(1,4,0)	7259.8	5.55(−5)	5281.2	5.07(−6)	5979.5	2.46(−5)
[1,0−] (5)	(0,5,1)	8376.5	1.79(−7)	6111.7	3.90(−8)	7655.2	5.61(−7)
[1,0+] (5)	(1,5,0)	8391.6	1.08(−5)	6113.4	1.02(−6)	6977.7	3.39(−7)
[1,0−] (6)	(0,6,1)	9490.6	8.69(−8)	6935.5	5.65(−9)	8636.1	8.40(−9)
[1,0+] (6)	(1,6,0)	9510.2	1.81(−7)	6939.6	1.93(−8)	7966.4	9.76(−9)
[1,0−] (7)	(0,7,1)	10590.9	1.77(−9)	7752.9	2.02(−10)	9607.1	1.31(−9)
[1,0+] (7)	(1,7,0)	10614.6	9.44(−9)	7759.4	7.95(−10)	8944.9	6.41(−10)
[2,0+] (1)	(2,1,0)	6307.7	4.37(−2)	4602.1	1.29(−2)	4780.9	4.03(−2)
[2,0−] (1)	(1,1,1)	6307.7	1.94(−1)	4603.9	5.28(−2)	5539.6	1.81(−3)
[1,1] (1)	(0,1,2)	6403.0	1.67(−4)	4654.2	1.07(−6)	6156.2	1.12(−1)

Table 3. (*continued*)

Local mode	Normal mode	H_2S		D_2S		HDS	
$[n_1, n_2](v_2)$	(v_1, v_2, v_3)	ω_{if}/ cm^{-1}	S_b/ $atm^{-1}cm^{-2}$	ω_{if}/ cm^{-1}	S_b/ $atm^{-1}cm^{-2}$	ω_{if}/ cm^{-1}	S_b/ $atm^{-1}cm^{-2}$
[2,0−] (2)	(1,2,1)	7451.5	3.27(−3)	5440.4	5.78(−4)	6542.8	3.86(−4)
[2,0+] (2)	(2,2,0)	7452.1	1.11(−5)	5439.6	1.70(−5)	5793.2	2.94(−4)
[1,1] (2)	(0,2,2)	7546.9	3.04(−6)	5490.1	4.06(−6)	7151.1	1.14(−3)
[2,0−] (3)	(1,3,1)	8585.3	8.55(−5)	6272.4	7.35(−6)	7539.0	2.48(−5)
[2,0+] (3)	(2,3,0)	8585.9	4.58(−5)	6272.2	7.78(−6)	6798.3	3.97(−5)
[1,1] (3)	(0,3,2)	8681.5	2.25(−5)	6321.7	2.00(−6)	8139.2	3.21(−5)
[2,0−] (4)	(1,4,1)	9707.9	9.54(−6)	7099.1	6.08(−7)	8527.4	4.28(−7)
[2,0+] (4)	(2,4,0)	9708.0	1.42(−6)	7099.3	7.80(−8)	7795.4	8.99(−7)
[1,1] (4)	(0,4,2)	9805.6	6.10(−7)	7148.4	2.48(−8)	9119.9	3.48(−6)
[2,0+] (5)	(2,5,0)	10817.4	5.91(−7)	7920.6	4.74(−8)	8783.7	7.11(−9)
[2,0−] (5)	(1,5,1)	10818.2	6.46(−10)	7920.3	2.65(−9)	9507.0	3.47(−8)
[1,1] (5)	(0,5,2)	10917.9	3.68(−7)	7969.9	1.54(−8)	10093.2	2.16(−8)
[3,0−] (1)	(2,1,1)	8723.0	7.77(−3)	6400.7	1.54(−3)	7384.0	2.29(−5)
[3,0+] (1)	(3,1,0)	8723.1	1.88(−3)	6400.6	3.72(−4)	8049.0	1.33(−5)
[2,1+] (1)	(1,1,2)	8906.9	1.15(−5)	6491.0	3.05(−6)	6578.0	1.13(−3)
[2,1−] (1)	(0,1,3)	8917.4	2.46(−6)	6507.8	3.62(−7)	8578.1	5.00(−3)
[3,0−] (2)	(2,2,1)	9847.8	2.32(−4)	7227.8	2.43(−5)	8376.9	1.54(−6)
[3,0+] (2)	(3,2,0)	9848.0	3.54(−7)	7227.8	1.96(−7)	9033.2	1.17(−5)
[2,1+] (2)	(1,2,2)	10037.4	4.00(−6)	7320.2	1.41(−6)	7580.3	1.10(−5)
[2,1−] (2)	(0,2,3)	10037.4	1.40(−6)	7331.9	4.61(−5)	9562.1	7.48(−5)

[a] These band origins are only accurate to $1\,cm^{-1}$.

Table 4. Vibrational absorption intensities, S_b, for the most intense bands, frequency ω_{if}, of LiNC calculated using various axis embeddings for the dipole surface. Effective band intensities calculated from the $J = 1 \leftarrow J = 0$ transitions are also provided for comparison.

		Absorption intensities/$atm^{-1}cm^{-2}$			
(v_s, v_b)	ω_{if}/cm^{-1}	Scattering	Eckart	$J = 1 \leftarrow J = 0$ calculation	ω_{if}/cm^{-1}
(0, 2)	247·2	5·53	5·53	6·83	248·1
(1, 0)	753·7	796·49	796·49	788·53	754·6
(2, 0)	1497·0	5·43	5·43	5·41	1497·9

References

[1] HERZBERG, G., 1960, *Infrared and Raman Spectra of Polyatomic Molecules* (Van Nostrand Reinhold).

[2] WILSON, E. B. JR., DECIUS, J. C., and CROSS, P. C., 1980, *Molecular Vibrations: The Theory of Infrared and Raman Vibrational Spectra* (Dover Publications).

[3] JENSEN, P., and SPIRKO, V., 1986, *J. molec. Spectrosc.*, **118**, 208.

[4] MILLER, S., TENNYSON, J., and SUTCLIFFE, B. T., 1989, *Molec. Phys.*, **66**, 429.

[5] CARTER, S., SENEKOWITSCH, J., HANDY, N. C., and ROSMUS, P., 1988, *Molec. Phys.*, **65**, 143.

[6] BOTSCHWINA, P., ZILCH, A., WERNER, H-J., ROSMUS, P., and E-A., REINSCH, 1985, *J. chem. Phys.*, **85**, 5107.

[7] SENEKOWITSCH, J., CARTER, S., ZILCH, A., WERNER, H-J., HANDY, N. C., and ROSMUS, P., 1989, *J. chem. Phys.*, **90,** 783.
[8] MILLER, S., TENNYSON, J., ROSMUS, P., SENEKOWITSCH, J., and MILLS, I. M., 1990, *J. molec. Spectrosc.*, **143,** 61.
[9] BROWN, R. D., BURDEN, F. R., and CUNO, A., 1989, *Astrophys.*, **347,** 885.
[10] BRUNET, J-P., FRIESNER, R. A., WYATT, R. E., and LEFORESTIER, C., 1988, *Chem. Phys. Lett.*, **153,** 425.
[11] ECKART, C., 1935, *Phys. Rev.*, **47,** 552.
[12] BUNKER, P. R., 1979, *Molecular Symmetry and Spectroscopy* (Academic Press).
[13] BRINK, D. M., and SATCHLER, G. R., 1979, *Angular Momentum* (Oxford University Press).
[14] SUTCLIFFE, B. T., and TENNYSON, J., 1991, *Int. J. quant. Chem.*, **29,** 183.
[15] ZARE, R. N., 1988, *Angular Momentum* (John Wiley) §6.5.
[16] MEYER, W., BOTSCHWINA, P., and BURTON, P. G., 1986, *J. chem. Phys.*, **84,** 891.
[17] MILLER, S., TENNYSON, J., and SUTCLIFFE, B. T., 1990, *J. molec. Spectrosc.*, **141,** 104.
[18] TENNYSON, J., and SUTCLIFFE, B. T., 1984, *Molec. Phys.*, **51,** 887.
[19] ESSERS, R., TENNYSON, J., and WORMER, P. E. S., 1982, *Chem. Phys. Lett.*, **89,** 223.
[20] BROCKS, G., TENNYSON, J., and VAN DER AVOIRD, A., 1984, *J. chem. Phys.*, **80,** 3223.
[21] HENDERSON, J. R., and TENNYSON, J., 1990, *Molec. Phys.*, **69,** 639.
[22] DINELLI, B. M., MILLER, S., and TENNYSON, J., 1992, *J. molec. Spectrosc.*, **153,** 718.
[23] LE SUEUR, C. R., HENDERSON, J. R., and TENNYSON, J., 1992, work in progress.